

Deuterium Inventory in Tore Supra : reconciling particle balance and post mortem analysis

E. Tsitrone, C. Brosset, B. Pégourié, E. Gauthier, J. Bouvet, J. Bucalossi, S. Carpentier, Y. Corre, E. Delchambre, L. Desgranges², D. Douai, A. Ekedahl, A. Escarguel⁵, Ph. Ghendrih, C. Grisolia, A. Grosman, J. Gunn, S.H. Hong, W. Jacob³, F. Kazarian, M. Kocan, H. Khodja⁴, T. Loarer, Y. Marandet⁵, A. Martinez, M. Mayer³, O. Meyer, P. Monier Garbet, P. Moreau, J. Y. Pascal, B. Pasquet², F. Rimini, H. Roche, I. Roure², S. Rosanvallon, P. Roubin⁵, J. Roth³, F. Saint-Laurent, F. Samaille, S. Vartanian

Association Euratom CEA, CEA/DSM/IRFM, Cadarache, 13108 Saint-Paul-lez-Durance, France

² : CEA-DEN-CAD-DEC, CEA Cadarache, F-13108 Saint Paul-lez-Durance, France

³ : Max-Planck-Institute für PlasmaPhysik, Euratom Association, Boltzmannstr. 2, D-85748 Garching, Germany

⁴ : Laboratoire Pierre Süe, CEA-CNRS UMR 9956, CEA Saclay, 91191 Gif-sur-Yvette, France

⁵ : PIIM-UMR 6633 CNRS/Université de Provence, centre de St-Jérôme, 13397 Marseille, France

E-mail: emmanuelle.tsitrone@cea.fr

Abstract

Fuel retention, a crucial issue for next step devices, is assessed in present tokamaks using two methods : particle balance performed during shots and post mortem analysis carried out during shutdowns between experimental campaigns. Post mortem analysis generally gives lower estimates of fuel retention than particle balance. In order to understand the discrepancy between these two methods, a dedicated experimental campaign has been performed in Tore Supra to load the vessel walls with deuterium (D) and monitor the trapped D inventory through particle balance. The campaign was followed by an extensive post mortem analysis phase. This paper presents the status of the analysis phase, in particular the assessment of the D content in gap deposits. Indeed, using combined surface analysis techniques, it was possible to derive the relative contributions of different zones of interest on the Tore Supra limiter (erosion, thick deposits, thin deposits), showing that the post mortem inventory is mainly due to codeposition (90% of the total), in particular due to gap deposits. At the present stage of analysis, 50% of the inventory deduced from particle balance has been found through post mortem analysis, a significant progress with respect to previous studies (factor 8-10 discrepancy).

1. Introduction

Fuel retention in the vessel walls is a crucial issue for next step fusion devices, as the tritium inventory is limited for safety reasons. It could have a potential strong impact on the machine availability, if the maximum allowable tritium inventory is reached before the end of the planned plasma operation phase [1]. With its ability to perform discharges on relevant durations with actively cooled components, Tore Supra offers a unique opportunity to address these issues in true steady state from the plasma wall interactions point of view. This paper reports the recent progress achieved in this field, in the frame of the DITS project (Deuterium Inventory in Tore Supra), aimed at better understanding fuel retention in tokamaks.

To assess fuel retention, two methods are currently used in present devices :

- particle balance performed during the shot, deriving the wall inventory from measurements of the injected and exhausted particle fluxes
- post mortem analysis of samples retrieved from the vessel during shutdowns

Previous results on deuterium (D) retention in Tore Supra have shown that the wall inventory deduced from particle balance integrated over the experimental campaign is larger than deduced from post mortem analysis, as was found in most tokamaks [2] [3]. Moreover, the carbon (C) source eroded from the PFCs does not seem sufficient to account for the experimental retention rate through codeposition [2]. Therefore, another mechanism, diffusion of D towards the bulk of the PFC material, was investigated in laboratory experiments and has been evidenced for large fluence/exposure time on Carbon Fiber Composites (CFC) as used in

Tore Supra [4]. To progress further, the DITS project was launched, in order to understand the discrepancy between particle balance and post mortem analysis, and to identify the main retention mechanisms at stake. It includes 1) a dedicated experimental campaign 2) dismantling of selected PFCs to extract samples and 3) an extensive analysis phase in collaboration with European partners in the frame of the EU Plasma Wall Interaction Task Force.

In section 2, the experimental campaign, addressed in more details in [5], is briefly reviewed, with a focus on particle balance results. In section 3, sample extraction from the PFCs is described. In section 4, results from the post mortem analysis are presented, including consistency between the different techniques used. In section 5, the comparison between particle balance and post mortem analysis is discussed.

2. Particle balance during the experimental campaign

The aim of the experimental campaign was to load the vessel walls with a significant additional D inventory in a limited time before opening the machine for sample extraction and post mortem analysis. In order to do so, repetitive long pulses (2 minutes) based on a robust scenario ($I_p = 0.6$ MA, moderate lower hybrid (LH) power of 2 MW, medium density $n_e/n_{Gr} \sim 0.5$) were performed, allowing to run the equivalent of 1 year of operation within 2 weeks [5]. A carbonisation using ^{13}C and a boronisation were performed on day 1, to be used as markers of the beginning of the campaign during post mortem analysis (~ 80 monolayers deposited for each). Apart from this, 5 hours of plasma were carried out without any conditioning procedure. The main limitation came from bursts of radiation linked to “UFOs” originating from the vessel walls, potentially leading to disruptions [6] [7]. To overcome this difficulty, a second scenario at lower power (1.8 MW of LH, 80 s) and with a slower power ramp up was used at the end of the campaign, allowing to reach the objectives in terms of wall D loading.

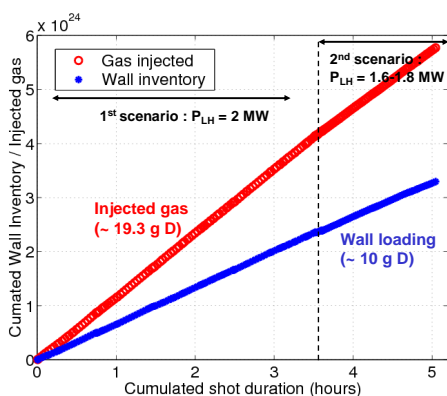


Fig 2 : cumulated gas injection and wall inventory for the DITS campaign

($\sim 2.5 \cdot 10^{22}$ D for nominal 120 s discharges). Most of it is recovered within the 2 minutes following the discharge, as can be seen from figure 1. Long term recovery (during nights and week ends) was also analyzed through a constant monitoring of the vessel pressure [5], and does not play a significant role in the overall particle balance (upper limit ~ 10 % of the trapped inventory, see table 1).

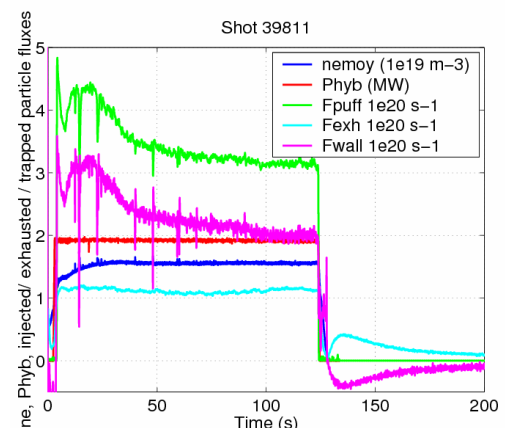


Fig 1 : particle balance for a typical shot of the DITS campaign

Particle balance, allowing to deduce wall retention from measurements of the injected and exhausted particle fluxes, is a reliable and accurate tool routinely used in Tore Supra (accuracy within ~ 10 % [8]). Typical results for a shot of the DITS campaign are illustrated in figure 1, where the injected (F_{puff}), exhausted (F_{exh}) and trapped (F_{wall}) particle fluxes are shown as a function of time, as well as the plasma density (n_{eoy}) and the lower hybrid power (P_{hyb}). The retention rate is found to be reproducible throughout the campaign, around $2 \cdot 10^{20}$

D/s in the stationary phase. For shots longer than ~ 1 minute, the release after shot ($2-4 \cdot 10^{21}$ D) is small compared to the inventory trapped during the shot

No sign of loss of density control or saturation of wall retention was observed during the campaign, as is seen in the linear evolution in figure 2, showing the injected gas and the trapped D inventory as a function of the cumulated plasma duration. The two scenario used during the campaign are indicated. A final D wall inventory of ~ 10.4 g ($3.1 \cdot 10^{24}$ D) was reached at the end of the campaign, corresponding to 53 % of the injected gas (~ 19.3 g or $5.8 \cdot 10^{24}$ D). This inventory is roughly 4 times larger than what was estimated as already present in the vessel, allowing to relate the results of the post mortem analysis phase mainly to the DITS campaign. Table 1 summarizes the cumulated injected and exhausted particle fluxes during the DITS campaign.

Injected	Exhausted				Wall Inventory
	During shots	After shots	Long term	Total	
$5.8 \cdot 10^{24}$ D	$1.8 \cdot 10^{24}$ D	$0.7 \cdot 10^{24}$ D	$0.2 \cdot 10^{24}$ D	$2.7 \cdot 10^{24}$ D	$3.1 \cdot 10^{24}$

Table 1 : cumulated injected flux, exhausted flux (during the shot, after the shot (within 2 minutes), long term and total), and resulting wall inventory during the DITS campaign.

3. Sample extraction after the DITS campaign

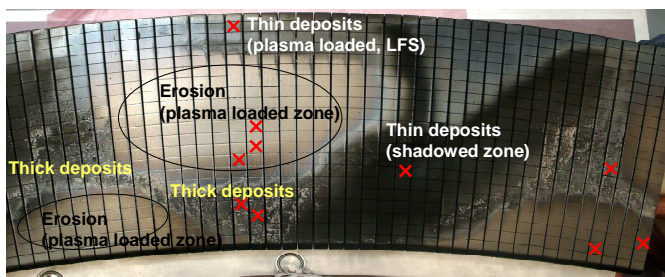


Fig 3a : sector Q6A of the Tore Supra limiter, extracted after the DITS campaign. The different zones of interest are indicated as well as the analysed tiles (crosses)

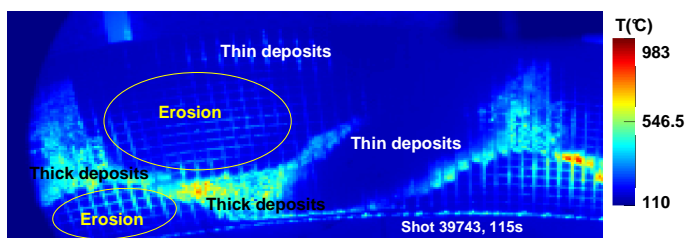


Fig 3b : IR imaging of the limiter sector during the DITS campaign. The different zones of interest are indicated

temperature and densities are low (around 10 eV and $5 \cdot 10^{17} \text{ m}^{-3}$ respectively from reciprocating Langmuir probe measurements). Deposits are also observed in the gaps between tiles, in particular in the erosion zone, as evidenced on the infrared imaging of the limiter shown on figure 3b for typical DITS conditions. The temperature of the tile surface in erosion zones is around 200°C , while the thin deposits in shadowed areas remain close to 120°C , the temperature of the cooling loop of Tore Supra plasma facing components. In contrast, the thick deposited layers, in shadowed zones or in gaps between tiles of the erosion zones, reach much higher temperature, around 500°C (NB : these temperatures are stationary during the discharge due to active cooling). In some limited areas, for thick deposits close to the plasma loaded zone, peaks up to 1000°C can be observed as seen on Figure 3b.

A sector of the main plasma facing component, the toroidal pump limiter (TPL), was then dismantled for analysis and is shown on figure 3a. The TPL is made of Carbon Fiber Composite (CFC) tiles, assembled on a copper heat sink. Different zones can be identified, correlated with the heat and particle fluxes pattern on the limiter [9] : erosion zones in the plasma loaded areas ($\sim 3.5 \text{ m}^2$), thin deposits zone in the far shadowed areas ($\sim 3 \text{ m}^2$), thick deposits at the boundary between plasma loaded and plasma shadowed zones ($\sim 0.5 \text{ m}^2$). Thin deposits are also observed on the low field side (LFS) of the limiter, although in a plasma loaded zone. However, it corresponds to a far SOL region (between 5-8 cm from the last closed flux surface radially), where the plasma electron

temperatures are low (around 10 eV and $5 \cdot 10^{17} \text{ m}^{-3}$ respectively from reciprocating Langmuir probe measurements). Deposits are also observed in the gaps between tiles, in particular in the erosion zone, as evidenced on the infrared imaging of the limiter shown on figure 3b for typical DITS conditions. The temperature of the tile surface in erosion zones is around 200°C , while the thin deposits in shadowed areas remain close to 120°C , the temperature of the cooling loop of Tore Supra plasma facing components. In contrast, the thick deposited layers, in shadowed zones or in gaps between tiles of the erosion zones, reach much higher temperature, around 500°C (NB : these temperatures are stationary during the discharge due to active cooling). In some limited areas, for thick deposits close to the plasma loaded zone, peaks up to 1000°C can be observed as seen on Figure 3b.

A first analysis campaign was carried out on 10 limiter tiles (out of the 40 tiles extracted for DITS) selected in the 3 zones of interest : erosion (5 tiles), thin deposits (2 tiles, one in the far shadowed region, the other on the LFS of the limiter) and thick deposits (3 tiles). The analysed tiles are indicated on figure 3a. Samples were then cut from the tiles for the different analyses to be performed. Thermodesorption (TDS) was carried out to determine the global D content of the samples. In addition, Nuclear Reaction Analysis (NRA), using the $D(^3\text{He},p)\alpha$ reaction, and Secondary Ion Mass Spectrometry (SIMS) were performed on exposed surfaces of tiles as well as in gaps to determine the D profile as well as the impurity concentration within the samples.

Out of the 10 tiles, 7 were cut according to a standard procedure (roughly 1 quarter of tile devoted to TDS, NRA, SIMS respectively, while the last quarter was kept as a spare for further analysis if needed). Moreover, 2 mm thick slices were cut within the NRA and TDS quarters, from the plasma facing surface of the tile down to the surface attached to the heat sink, in order to study the D penetration in the bulk material. Only the top plasma facing and the middle slices were studied, as the last slice contains copper infiltrations from the assembly process with the heat sink. 3 tiles (1 for every zone of interest) were then cut according to a refined procedure, in order to study detailed features, such as poloidal versus toroidal gaps for instance. It has to be noted that the TDS samples cut following the standard method include deposits on 1 toroidal gap out of the 4 lateral sides of the sample, while the TDS samples cut following the refined procedure do not include any gap surfaces. Therefore, TDS will give the global D content of the samples, but without being able to discriminate D coming from gap deposits and tile surface for standard samples. Only samples cut with the refined procedure will allow to assess the tile contribution only. Refined samples are signaled in the paper by ** (see abscissa in figures 4 to 6). On the other hand, NRA will give the D distribution profile on the tile surface and in the gaps (and by integration the global D content), but will be limited in the analyzed depth (maximum depth $\sim 40 \mu\text{m}$ with the highest NRA beam energy $E(^3\text{He}) = 6 \text{ MeV}$). It will therefore miss the contribution of deeply trapped D in the bulk material or in thick deposited layers. In the following analysis, results from both methods are then combined to derive a global D content, NRA being used to estimate the contributions from the gaps on TDS samples, while TDS is used to account for deeply trapped D not seen by NRA.

4. Post mortem analysis of the DITS samples

4.1 Global D content from TDS

The global D content was measured with TDS for the top (plasma facing) and the middle (2 mm below) samples, as shown on figure 4 (NB : sample surface $\sim 0.8 \text{ cm}^2$). The sample temperature was increased with a well controlled temperature ramp of 1°C/s up to 1200°C for the top samples. For the middle samples, the temperature was limited to 900°C due to the presence of copper from the heat sink. The measurements presented here are corrected by renormalizing the H_2 and HD peaks (additional 30% contribution to account for the particles not yet desorbed at 900°C , as deduced from of the TDS spectra on the top samples).

In erosion zones, surface content up to $\sim 10^{23} \text{ D/m}^2$ were measured on the top samples, much higher than what would be expected from saturation of the implanted layers within the incident particles penetration range ($\sim 10^{21} \text{ D/m}^2$ [10] for typical DITS conditions, with $\sim 300 \text{ eV}$ - 1 keV incident energy). D was also detected in the middle samples, 2 mm below the plasma exposed surface, although a factor 15-30 lower. In deposition zones, $\sim 10^{23} \text{ D/m}^2$ to $5 \cdot 10^{23} \text{ D/m}^2$ were measured for thin and thick deposits respectively. However, one should be cautious when translating the sample D content measured by TDS into surface concentration, as the standard samples include both the tile surface and gap deposits (see section 5 for concentrations corrected from this effect through combined NRA and TDS analysis). Indeed,

the samples without gap deposits (marked with ** on the abscissa) exhibit a lower D content in erosion and thick deposition zones (although within error bars for top samples, more visible on middle samples where the contribution of the tile itself is expected to be smaller). This is consistent with the visual inspection of the limiter, showing gap deposits mainly in these two zones. It is also consistent with NRA analysis of the D content in gaps presented in section 4.2, showing very low D concentrations in gaps of the thin deposits zone compared to the erosion and thick deposits zones.

In all cases, roughly 2/3 of the D content is desorbed as D_2 or HD molecules, while the remaining 1/3 is desorbed as hydrocarbons, mainly CD_4 and CD_3H . Higher masses are also detected in the TDS spectra, but are difficult to disentangle. In any case, their contribution to the overall D content is small.

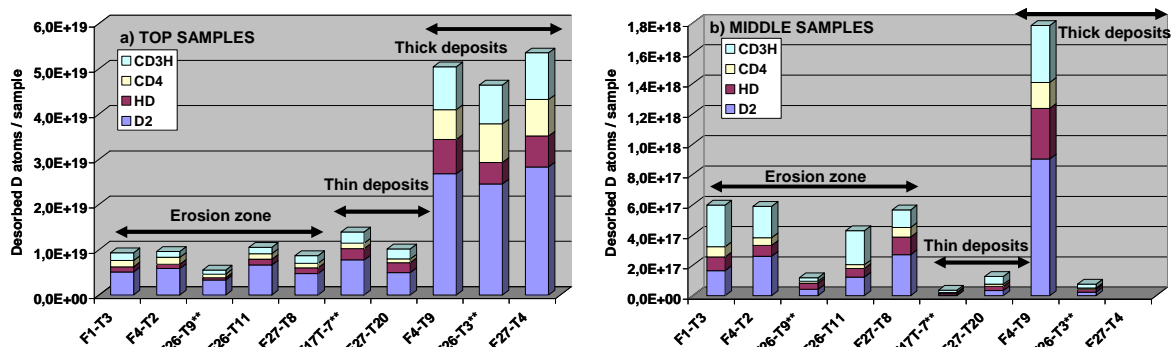


Fig 4 : D sample content as a function of sample identification number as measured from TDS for (a) top samples and (b) middle samples. Samples with ** correspond to the refined cutting procedure (NB1 : sample surface $\sim 0.8 \text{ cm}^2$, NB2 : for middle samples, F27-T4 could not be measured)

4.2 NRA measurements

A comprehensive NRA analysis campaign was performed in collaboration with IPP Garching, in the frame of the EU PWI TF (> 350 NRA spectra on ~ 60 samples extracted from the 10 limiter tiles). Four energies of the ^3He beam were used (from 800 keV to 6 MeV) in order to derive the D profile up to several tens of microns deep into the samples [11]. A first study on uniformity of D concentration within a given sample (measurements every mm at a given beam energy) was undertaken. For low beam energy (800 keV, corresponding to an analyzed depth $\sim 1.5 \mu\text{m}$), the standard deviation is 10-20% for all zones (erosion, thin or thick deposits). However, at higher energies, standard deviations as high as 30-50 % can be reached (but applying to lower absolute D concentration deeper in the sample). This underlines the non uniformity of the local D concentration deep in the material at the scale probed by NRA ($\sim 1 \text{ mm}^2$ beam size) and could be linked to the porosity network of CFC [12].

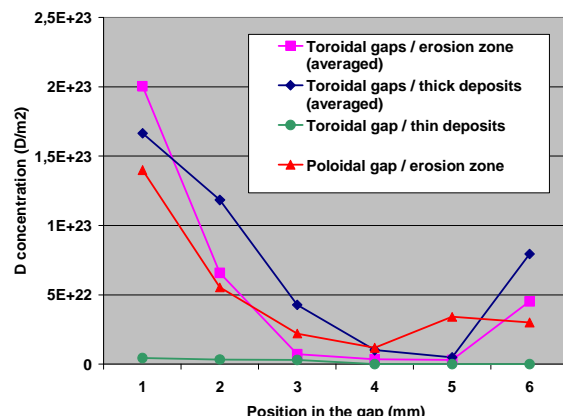


Fig 5 : D concentration measured by NRA in toroidal gaps for the erosion, thick deposits, thin deposits zones. Results from a poloidal gap in the erosion zone are also shown.

The D concentration measured by NRA at the tile surface has been presented in [5]. Lateral faces of the tiles have also been analyzed to study the D distribution in gaps between tiles. Results are shown on figure 5, where the measured D concentration is plotted against the position in the gap, from 1 mm from the plasma facing surface down to 6 mm (position of the

heat sink). For toroidal gaps in the erosion and thick deposition zones, results have been averaged on 5 and 3 samples respectively, while for thin deposits and the poloidal gap in erosion zone, only one measurement is available so far. The erosion and thick deposits zone exhibit similar D concentrations in gaps, with values up to $1.5\text{-}2 \cdot 10^{23} \text{ D/m}^2$ close to the plasma surface, typical of values measured in other deposited layers on the limiter (see section 4.1 and [5]). In contrast, the D concentration in gaps of the thin deposits zone is much lower. A preliminary comparison between the toroidal and poloidal gaps in the erosion zones show no major difference. The D profile decays rapidly in the gaps (within 2-3 mm), as was found in other tokamaks. The fact that values deep in the gap ($> 5 \text{ mm}$) seem to increase again could be due to a surface temperature effect (colder surface when getting closer to the heat sink) or to a measurement artifact, as samples were placed next to each other in the NRA sample holder. Due to the NRA beam size ($\sim 1 \text{ mm}^2$) and the precision on the exact location of the beam ($\sim 0.5 \text{ mm}$), the last data point could include contributions from both the deepest gap position (6 mm) of a given sample and the plasma closest gap position (1 mm) of the next sample. For the same reason, the first data point could be underestimated. However, this would not influence the integrated amount of D found in gaps.

4.4 Consistency of NRA and TDS measurements

To check the consistency from both methods, the TDS integral measurements have been reconstructed from the local NRA measurements for each top sample, adding top surfaces and gap contributions derived from NRA when applicable. To assess the gap contribution to the top TDS samples from the NRA

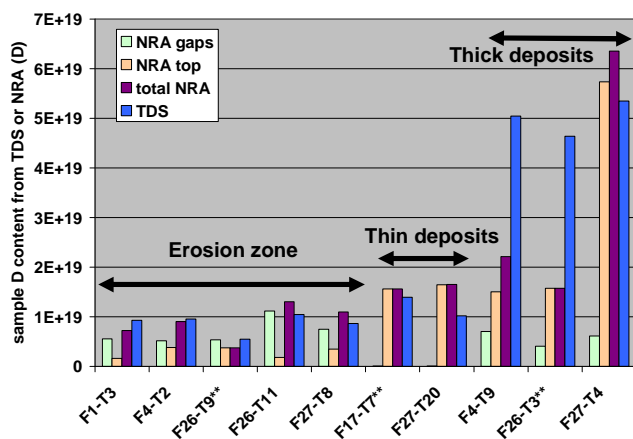


Fig 6 : Comparison between sample D content from TDS measurements and reconstructed from NRA, adding top surface and gap contributions.

measurements, the spatial gap distribution on the first 2 mm has been taken into account and applied to the relevant surface of the TDS sample (toroidal gap 10 mm x 2 mm). Results are shown on figure 6. Both methods are in fair agreement in the erosion zone and in the thin deposits zone. Taking into account the gap contribution is an essential factor to get a good agreement between NRA and TDS in the erosion zone, while the impact is small in the thin deposits zone where the gap D

concentration is much lower. However, the gap contribution is not enough to reconcile both methods in the thick deposits zone. In general, NRA gives a lower D content than

TDS, which is consistent with the fact that NRA does not see D trapped deeper than $\sim 40 \mu\text{m}$. The only exception is for tile F27-T4, where NRA exceeds TDS, as well as values from other samples in the thick deposited layers. More statistics would be needed to clarify this point.

TDS and NRA can then be combined to discriminate the D content in the tile and in gap deposits. Indeed, the tile surface D concentration can be derived from :

- method 1 : TDS analysis of the refined cutting sample (but poor statistics, with only 1 sample/zone available)
- method 2 : NRA analysis of the tile surface (but will underestimate the concentration if the D content beyond $30 \mu\text{m}$ is significant)
- method 3 : Combined TDS analysis of the standard samples (including the tile surface and 1 gap) and NRA analysis of the gap concentration. The gap contribution derived

from NRA is then subtracted from the TDS global D content to obtain the tile surface contribution.

Results for the 3 methods are summarized in table 2. The gap concentrations are derived from NRA, averaged over the spatial distribution in the gap. As a first step, results are also averaged over the available samples for each zone, assuming comparable D content in a given zone, as seem to indicate the data from the 10 tiles analysed so far.

		Erosion zone	Thin deposits	Thick deposits
Gap deposits D concentration (NRA, averaged over the 6 mm gap profile) (D/m^2)		$1.4 \cdot 10^{23} \pm 4.5 \cdot 10^{22}$	$3.3 \cdot 10^{21} \pm 6 \cdot 10^{20}$	$1.1 \cdot 10^{23} \pm 2.8 \cdot 10^{22}$
Tile D concentration (D/m^2)	1 : TDS refined	$6.8 \cdot 10^{22}$	$1.7 \cdot 10^{23}$	$5.7 \cdot 10^{23}$
	2 : NRA tile	$3.6 \cdot 10^{22} \pm 1.3 \cdot 10^{22}$	$1.9 \cdot 10^{23} \pm 3.3 \cdot 10^{22}$	$3.6 \cdot 10^{23} \pm 3 \cdot 10^{23}$
	3 : combined TDS + NRA	$3 \cdot 10^{22} \pm 4.2 \cdot 10^{22}$	$1.2 \cdot 10^{23} \pm 5.6 \cdot 10^{19}$	$5.7 \cdot 10^{23} \pm 4.5 \cdot 10^{22}$

Table 2 : Estimate of D concentration (D/m^2) in gaps and tile surface of the different zones of interest. The tile surface contribution is assessed from the 3 methods described in the text. When applicable (ie several measurements available), the standard deviation is given

For the thin deposits zone, where the gap contribution is negligible, methods 1, 2 and 3 are in reasonable agreement for the assessment of the tile surface concentration. For the calculation of the global inventory of section 5, an average between the 3 methods is taken ($1.6 \cdot 10^{23} D/m^2$). For the thick deposits zone, methods 1 and 3 are in fair agreement, while method 2, based on NRA only, underestimate the tile D concentration, as expected due to the thickness of the deposited layers, larger than the NRA information depth. For section 5, the value given by methods 1 and 3 is taken ($5.7 \cdot 10^{23} D/m^2$). For the erosion zone, the assessment is more difficult due to the large error bars on the gap contribution, which is dominant in this case. The fact that NRA based estimates (method 2) are below TDS based estimates (method 1) could again indicate D trapping beyond the NRA range in the sample, due to bulk diffusion of D in the tile. For section 5, an average between the 3 methods is taken ($4.5 \cdot 10^{22} D/m^2$).

5. Comparison of particle balance and post mortem analysis

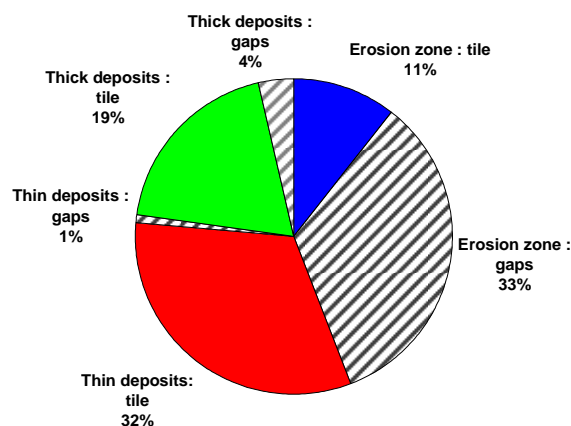


Fig 7 : Contribution of the different zones (erosion, thin deposits, thick deposits) to the overall wall inventory deduced from post mortem analysis. For each zone, the contribution of the gap deposits and the tile is indicated.

From all of the above, an integrated wall inventory from post mortem analysis can be computed and compared to particle balance for the DITS campaign. The gap deposits contribution is estimated from NRA measurements as shown in table 2, while the tile contribution is assessed from averaging between the different methods combining TDS and NRA as described in section 4.4. Results are shown on figure 7.

The erosion ($3.5 m^2$), thin deposits ($3 m^2$) and thick deposits ($0.5 m^2$) zones contribute for 44, 33 and 23 % of the total respectively. The distribution between gap deposits and tile contribution is very different depending on the zone. Indeed, in the erosion zone, the gap deposits are the main contribution (~ 75 % of the total in the zone), while in the thin deposits zone, they play no role (less than 2 % of the total in the zone). In the thick deposits zone, the situation is intermediate (~ 15 % of the total of the zone in gap deposits).

As far as retention mechanisms are concerned, results from the post mortem analysis presented in this study would lead to 90 % of the wall inventory related to codeposition (in the thin and thick deposits zone as well as in the gap deposits of the erosion zone). This fraction could still be increased by taking into account deposited layers not yet analyzed on the TPL (leading edge) or on other PFCs (inner bumpers) when results become available. However, it remains that the D concentration in tile surface in erosion zones is still significant and higher than expected from simple implantation. This could be linked to the porosity network of the CFC tiles [5] [13].

The total wall inventory deduced from post mortem analysis at the present stage of the analysis phase is $\sim 1.5 \cdot 10^{24}$ D (error bars estimated to be $\pm 15\%$), ie $\sim 50\%$ of the $3.1 \cdot 10^{24}$ D derived from the particle balance. This represents a significant progress with respect to previous studies [14], showing that a dedicated experimental campaign and an extensive analysis phase are required to reconcile both methods. In particular, performing particle balance on specific shots (in general high performance shots) and post mortem analysis for campaign averaged conditions makes the comparison difficult, as has been underlined in [15].

6. Summary

In order to better assess fuel retention in tokamaks, it is essential to understand discrepancies between the two measurements methods currently used, particle balance and post mortem analysis. In order to tackle this issue, a dedicated experimental campaign to load the vessel walls with D has been performed in Tore Supra, followed by an extensive post mortem analysis phase. This paper presents the status of the analysis phase, in particular the assessment of the D content in gap deposits. Indeed, using combined surface analysis methods (local measurements with NRA and integrated measurements with TDS), it was possible to derive the relative contributions of different zones of interest on the limiter (erosion, thick deposits, thin deposits), showing that the post mortem inventory is mainly due to codeposition (90% of the total), in particular due to gap deposits. At the present stage of analysis, 50% of the inventory deduced from particle balance has been found through post mortem analysis, a significant progress with respect to previous studies (factor 8-10 discrepancy). In order to progress further, future work will include the analysis of deposited layers not yet studied, in particular on the TPL leading edge as well as on other PFCs, such as the inner bumpers.

References

- [1] : J. Roth et al., 18th International Conference on Plasma Surface Interactions, Toledo (2008), to be published in *J. Nucl. Mater.*
- [2] : E. Tsitrone, *J. Nucl. Mater.* **363–365** (2007), p. 12
- [3] : T. Loarer et al., *Nucl. Fusion.*, **47** (2007), p 1112
- [4] : J. Roth et al., *J. Nucl. Mater.* **363–365** (2007), p. 822
- [5] : B. Pégourié et al., 18th International Conference on Plasma Surface Interactions, Toledo (2008), to be published in *J. Nucl. Mater.*
- [6] : A. Ekedahl et al., 18th International Conference on Plasma Surface Interactions, Toledo (2008), to be published in *J. Nucl. Mater.*
- [7] : A. Ekedahl et al., these proceedings
- [8] : J. Bucalossi et al., *J. Nucl. Mater.* **363–365** (2007), p. 759
- [9] : R. Mitteau et al., *Nucl. Fusion* **46** No 3 (March 2006) S49-S55
- [10] : K. L. Wilson et al., in Atomic and plasma-material interaction data for fusion, supplement to *Nucl Fusion*, IAEA, Vienna, 1991
- [11] : M. Mayer et al., submitted to *Nucl. Instr. Meth. B*
- [12] : N. Bernier et al., submitted to *J. Nucl. Mater*
- [13] : C. Martin et al., 18th International Conference on Plasma Surface Interactions, Toledo (2008), to be published in *J. Nucl. Mater.*
- [14] : C. Brosset et al., *J. Nucl. Mat.* **337–339** (2005) 664
- [15] : T. Loarer et al, 18th International Conference on Plasma Surface Interactions, Toledo (2008), to be published in *J. Nucl. Mater.*